336–349 *Nucleic Acids Research, 2018, Vol. 46, No. 1* *Published online 10 November 2017*
doi: 10.1093/nar/gkx1105

C/EBPβ mediates RNA polymerase III-driven transcription of oncomiR-138 in malignant gliomas

Federica Di Pascale[1,2], Srikanth Nama[1], Manish Muhuri[1], Shan Quah[1], Hisyam M. Ismail[1], Xin Hui Derryn Chan[1], Gopinath M. Sundaram[1], Rajkumar Ramalingam[1], Brian Burke[1] and Prabha Sampath[1,2,3,*]

[1]Institute of Medical Biology, Agency for Science Technology & Research (A*STAR), Singapore 138648, Singapore, [2]Department of Biochemistry, Yong Loo Lin School of Medicine, National University of Singapore, Singapore and [3]Program in Cancer and Stem Cell Biology, Duke-NUS Medical School, 8 College Road, Singapore 169857, Singapore

Received June 11, 2017; Revised October 21, 2017; Editorial Decision October 23, 2017; Accepted October 24, 2017

ABSTRACT

MicroRNA-138 (miR-138) is a pro-survival oncomiR for glioma stem cells. In malignant gliomas, dysregulated expression of microRNAs, such as miR-138, promotes Tumour initiation and progression. Here, we identify the ancillary role of the CCAAT/enhancer binding protein β (C/EBPβ) as a transcriptional activator of miR-138. We demonstrate that a short 158 bp DNA sequence encoding the precursor of miR-138-2 is essential and sufficient for transcription of miR-138. This short sequence includes the A-box and B-box elements characteristic of RNA Polymerase III (Pol III) promoters, and is also directly bound by C/EBPβ via an embedded 'C/EBPβ responsive element' (CRE). CRE and the Pol III B-box element overlap, suggesting that C/EBPβ and transcription factor 3C (TFIIIC) interact at the miR-138-2 *locus*. We propose that this interaction is essential for the recruitment of the RNA Pol III initiation complex and associated transcription of the oncomiR, miR-138 in malignant gliomas.

INTRODUCTION

Malignant gliomas are highly aggressive forms of brain Tumour, associated with high rates of mortality. Despite surgical advances and progress in adjuvant therapies, high-grade gliomas remain difficult to treat and often carry poor prognoses (1). Overcoming these therapeutic challenges necessitates an understanding of the underlying factors governing tumour growth and survival.

Initiation and progression of malignant gliomas have been linked to alterations in microRNA (miRNA) expression. We have previously demonstrated that miR-138 is a pro-survival oncomiR for glioma stem cells (GSCs). Depletion of miR-138 in GSCs has a dual effect on tumour cell population through a sharp reduction in cell proliferation and a simultaneous increase in apoptosis (2). However, the molecular mechanisms behind this aberrant expression remain poorly defined.

Human miR-138 (hsa-miR-138) is encoded by two intergenic *loci* on chromosomes 3 and 16, which encode two putative precursors of miR-138, known as 'pre-miR-138-1' and 'pre-miR-138-2' (3,4). However, only pre-miR-138-2 shows overall conservation of synteny amongst different vertebrate species in multiple sequence alignments of the two chromosomal regions and generates mature miR-138 in brain tissue (5). Expression analysis of the two transcripts in GBM cell lines could only detect pre-miR-138-2 (2). Here, we focus on pre-miR-138-2, which generates mature miR-138 and characterize the transcriptional regulation of miR-138-2.

We identify the leucine-zipper transcription factor CCAAT/enhancer binding protein β (C/EBPβ) as a transcriptional activator of miR-138. We demonstrate that a short DNA sequence of 158 bp is sufficient for miR-138 transcription, and that this sequence harbours a 'C/EBPβ responsive element' (CRE), which is directly bound by C/EBPβ. We also present the first comprehensive evidence for transcription of a microRNA gene by RNA Polymerase III (Pol III) and propose a model whereby C/EBPβ coordinates the recruitment of the Pol III initiation complex.

MATERIALS AND METHODS

Cell culture

Human Glioblastoma cell lines U-87 MG and U-251 MG were maintained in Minimum Essential Medium (MEM) supplemented with 10% fetal bovine serum (FBS), 5% penicillin/streptomycin, 2 mM L-glutamine, and 1 mM sodium pyruvate. HEK-293T cells were routinely passaged in Dulbecco's Modified Eagle Medium (DMEM) supplied

*To whom correspondence should be addressed. Tel: +65 6407 0171; Email: prabha.sampath@imb.a-star.edu.sg

with 10% FBS, 2 mM L-glutamine, and 1 mM sodium pyruvate. GBM patient-derived cell line IMB-1 was obtained using an institutional review board-approved protocol and cultured in chemically defined serum-free selection growth medium with 1 ng/ml basic fibroblast growth factor (bFGF), 1 ng/ml epidermal growth factor (EGF), 5 μg/ml Heparin, 100 × Pen-strep/Glutamine (PSQ), 100 × Glutamax media, serum-free supplement (B27) in a 3:1 mix of Dulbecco's modified Eagle's medium (DMEM), and Ham's F-12 Nutrient Mixture (F12). Cultures were incubated at 37°C and 5% CO_2 with growth factor replenishment. Neurosphere cultures were expanded by mechanical trituration.

Preparation of lentiviral stocks and transduction

Two independent shRNA sequences specifically targeting C/EBPB (Sh1, CGACTTCCTCTCCGACCTCTT; Sh2, GAAGACCGTGGACAAGCAC) or the mature antimiR-138 sequence (CGGCCTGATTCACAACACCAGCT) were cloned into a lentiviral vector under the human promoter H1, while the reporter gene CopGFP was expressed under the human PGK promoter. To produce third-generation lentiviruses, Lenti-X 293T cells (Clontech) were transfected with maxiprep DNA constructs, prepared using Plasmid Maxi Kit (Omega bio-tek), and lentiviral packaging mix (Addgene) made of three constructs: pMDLg/pRRE (#12251), pRSV-Rev (#12253), and pMD2.G (#12259). The lentiviral shRNA constructs were transduced in U-87 MG cells along with a scrambled control. Three days post-transduction, successful viral infection was detected by GFP expression and cells were harvested for RNA isolation and protein lysate preparation.

Quantitative RT-PCR

RNA was isolated from cells using miRCURY RNA Isolation Kit (Exiqon). cDNA was synthesized from small non-coding RNA using a miRNA RT assay (TaqMan). Expression levels of miRNA were measured on a 7900 fast RT-PCR system (Applied Biosystems) in triplicates using 1 ng/μl cDNA and TaqMan probes specific for miR-138. U6 probe was used as an endogenous control. The ΔΔCt method was applied to determine the transcript abundance. For cDNA preparation from total mRNA, SuperScript III Reverse Transcriptase was used. Quantitative Real Time PCR (qRT-PCR) analyses were performed using two pairs of primers that amplify a coding region of C/EBPβ or target gene. qRT-PCR was performed in triplicates with SYBRgreen mix (Applied Biosystems), 0.25 uM primers and 1 ng/μl cDNA.

Western blotting

Cell lysates were prepared from U-87 MG and U-251 MG cells and resolved on 4–15% Criterion TGX Precast Gels (Bio-Rad). PVDF membranes (Millipore) were used for protein transfer. Immunoblots were probed with a primary antibody raised against C/EBPβ (C-19): sc-150 (Santa Cruz; 1:1000), followed by anti-rabbit HRP (Santa Cruz; 1:4000). All blots were stripped and probed with Mouse Anti-Hsp90 antibody (BD Transduction Laboratories, 1:5000) as loading control.

Cell proliferation and Caspase 3/7 assays

U-87 MG cells were transduced with either scrambled control or C/EBPβ shRNA or antimiR-138. 150 cells per well were seeded in 96 well-plates in complete medium. Cell proliferation or Caspase 3/7 activity were measured at different days post seeding using respectively the kits CellTiter-Glo® Luminescent Cell viability assay (Promega) and Caspase-Glo® 3/7 Assay Systems (Promega). Both the assays were performed as per manufacturer's instructions using a luminometer. Experiments were performed in two biological replicates with at least eight technical replicates per condition.

Electrophoretic mobility shift assay (EMSA)

A 158 bp miR-138 promoter region was amplified and labelled with radioactive [γ-32P] ATP. The DNA probe was purified with phenol:chloroform:isoamyl alcohol (25:24:1) and then eluted in 600 μl elution elution buffer by gel filtration (Illustra MicroSpin G-25 columns, GE Healthcare). Binding reactions were carried out in a total volume of 30 μl containing 24 ng/μl nuclear extract from LAP-overexpressing 293T or from WT 293T, radiolabeled oligonucleotides in 2 × binding buffer [10 mM HEPES pH 7.5, 50 mM KCl, 2.5 mM $MgCl_2$, 0.5 mM DTT, 10% glycerol, 1 μg/ml BSA] and 6 μg/μl non-specific competitor poly (dI-dC). The reaction mixture was incubated for 30 min on ice, followed by electrophoresis in an 8.5–12% native gel for 1 h at 136 V. The gel was dried and exposed overnight to an X-ray film (Thermo Scientific). Supershift of the specific DNA/protein complex was performed by addition of 0.5 μg/μl monoclonal anti-FLAG M2 antibody (F3165 SIGMA).

Chromatin immunoprecipitation (ChIP)

Chromosomal DNA preparation was performed as described by Squazzo *et al.* (2006). Briefly, chromosomal DNA was prepared from 3×10^6 U-87 MG cells, fixed with 40 μl of 37% formaldehyde to a final concentration of 1.5%, and incubated for 15 min at room temperature. The excess of formaldehyde was neutralized by addition of 141 μl 1 M glycine/ml of medium for 5 min. Cells were then washed with 15 ml ice cold 2 × PBS and centrifuged at 2000 × *g* for 5 min. The pellet was suspended and incubated for 30 min in 100 μl/1×10^6 cells of Buffer A (10 mM HEPES pH 7.9, 10 mM KCl, 0.1 mM EGTA, 1 mM DTT, 0.5 mM PMSF) supplemented with 1 × Roche protease inhibitor cocktail and 10% glycerol. Cells were then treated with 75 μl 10% NP-40 and centrifuged at 1500 × *g* for 5 min. The pellet was suspended in 2 ml ChIP buffer (50 mM Tris pH 7.4, 150 mM NaCl, 5 mM EDTA, 0.5% NP-40, 1% Triton X-100, 0.05% SDS, 1 × Roche Inhibitor cocktail) and 400 μl lysate was aliquoted into chilled 1.5 ml Eppendorf tubes. Appropriate sonication conditions were determined to cleave genomic DNA into 200 bp-500 bp fragments (12 pulses of 30 s each). ChIP Buffer (250 μl) was then added to each Eppendorf

tube containing the specific antibody for the immunoprecipitation. The antibodies used were as follows: rabbit control IgG (vector Labs-W0121 – 1 μl), anti- C/EBPβ (H-7X, sc-7962, Santa Cruz – 2 μg), anti-POLR3D, (A302-295A, Bethyl Laboratories – 2 ug), anti-POLR3C (H00010623-B03P, Abnova – 2 ug), anti-POLR3E (B-11, sc-365703, Santa Cruz – 2 ug), anti-TFIIIC102 (sc-393235, Santa Cruz – 2 ug) anti-BRF1 (A301-227A, Bethyl Laboratories – 2 ug). The binding reaction was carried out overnight at 4°C in a rotator shaker. The next day, samples were centrifuged at max speed for 10 min. Protein A sepharose beads (Amersham Sepharose 4LB) were incubated in 0.5% BSA in PBS for 30 min and then washed with ChIP buffer. Protein A sepharose beads (100 μl) were added to the immunoprecipitated samples and incubated for 1 h at 4°C. The samples were then centrifuged for 30 min at max speed and washed six times with 500 μl ChIP buffer and once with cold PBS. Upon removal of PBS, 100 μl Chelex-100 slurry (BioRad) was added to the samples and incubated at 95°C for 5 min. The samples were then centrifuged at max speed for 5 min and the first DNA elution was collected. To collect the second elution, 120 μl of nuclease-free water was added to the samples. RNase A (1 μl; Fermentas) was added to the DNA elution and incubated for 2 h at 37°C. To isolate the input DNA, 350 μl of cell lysates were treated and incubated for 2 h at –20°C with 35 μl 3M sodium acetate and three volumes of 100% ethanol. Input samples were centrifuged at max speed for 10 min at 4°C and washed with 500 μl of 70% ethanol. After removing the ethanol from the pellet, the input sample was treated with Chelex-100 slurry and processed as described for the immunoprecipitated samples. Protein/DNA cross-links were reversed by treating the samples (including input) with 5 μl RNase A for 2 h at 37°C. Proteinase K (5 μl) was then added to the samples and incubated overnight at 55°C. The DNA was eluted in 40 μl nuclease free-water using the QIAquick PCR purification kit. Three microliters of input samples were then loaded onto a 1.5% agarose gel to check for the presence of a DNA smear between 200 bp and 500 bp. SYBR green-based qPCR analysis was performed with 4 μl DNA (diluted 6-fold) of each immunoprecipitated sample or input chromatin. Primers used to amplify the genes are detailed in Supplementary Table S1. Fold enrichment of the target sequences was calculated using the ΔΔCt method with normalization to negative control IgG.

Dual-Luciferase assay

The luciferase vector pGL4.23 luc2/minP (Promega, E8411) was used to express six deletion fragments of the miR-138 promoter region, which bears a total of six C/EBPβ binding sites. U-87 MG or U-251 MG cells (0.1 $\times$ 10^6/well) were plated in a 12-well plate and transfected the next day with 1.25 μg/μl empty reporter vector (control) and 50 ng/μl of the normalization vector pCMV (Renilla Luciferase) along with 1.25 μg/μl of miR-138 deletion constructs (from P1 to P6) using 3 μl/well of Fugene HD (Promega). U-87 MG or U-251 MG cells were lysed 24 h post-transfection using Passive Lysis Buffer (Dual-Luciferase Reporter Assay System, Promega) according to the manufacturer's instructions. Firefly luciferase activity was measured with a luminometer and the signal was normalized to Renilla luciferase activity signal.

Mutagenesis of the CRE element

Site-directed mutagenesis of the CRE element was performed with the QuickChange II XL Site-Directed Mutagenesis Kit (Agilent Technologies) following the manufacturer's instruction. Briefly, DNA strand synthesis of mutant CRE was achieved by amplifying the pJET1.2 plasmid containing wild-type miR-138 promoter sequence (P6) with specific primers (Supplementary Table S1). Following the amplification of the mutant strand, the methylated parental DNA was digested with the restriction enzyme DpnI. The digested products were then subjected to transformation, miniprep and sequencing to check the presence of mutations in the CRE element.

5′ RACE rapid amplification of cDNA ends

To identify the miR-138 primary transcript and transcription start site, 5′ rapid amplification of cDNA ends (5′ RACE) was performed using the SMARTer race kit (Clontech). Reactions were performed according to manufacturer instructions. The first strand synthesis was carried out using random degenerative primers instead of oligodT. Briefly, 1 ug of RNA was isolated from Drosha knock down U87MG cells to enrich for pri-miRNA transcripts and subjected to 5′ RACE. Next, PCR reactions were carried out using miR-138-2 specific reverse primer (5′-gtcgtgaaatagccgggtaagagg-3) and universal forward primer. PCR products were further cloned into blunt vector, pJET1.2 and sequenced to find out transcriptional start site of miR-138-2.

Treatment with RNA Pol II/III inhibitors

For RNA polymerases inhibitory studies, U-87MG cells were plated at the confluency of 50% for efficient drug inhibition. On the next day, cells were treated with specific drug inhibitors (DRB for polymerase II at 50 uM and RNA Polymerase III Inhibitor, CAS 577784-91-9, at 33 uM and 66 uM) for 19 h. General RNA Pol-II inhibitor α-amanitin was used at 2 uM concentration. After treatment, cells were harvested and RNA was isolated for qRT-PCR analysis.

Intracranial implantation of U-87 MG cells

Intracranial transplantation of U-87 MG cells into six-month-old NOD/SCID/IL2rg mice (Jackson Laboratory) was performed in accordance with an Institutional Animal Care and Use Committee-approved protocol. Luciferase-expressing U-87 MG cells bearing either C/EBPβ shRNA or scrambled control were orthotopically transplanted following washing and re-suspension in PBS. A total of 0.1 $\times$ 10^6 cells in a 3 μl volume were injected stereotactically into the striatum of immunodeficient mice, which were maintained until the development of neurological symptoms. To monitor cell survival upon implantation, mice were imaged using the IVIS Spectrum Imaging System (Xenogen) upon injection of Luciferin. Bioluminescence signals were analyzed using Living Image software (IVIS Living Image

v3.0). Brain tissue collected from the euthanized mice was fixed in 4% PFA, embedded and sectioned, and subjected to H&E staining.

miR-138 *in situ* hybridization

Five-micron sections were processed and boiled in pretreatment solution (Panomics), washed in PBS and treated with protease (Panomics) at 37°C. Sections were incubated with LNA probes (5′ DIG-labeled LNA probes specific for miR-138 or scrambled probe with no homology to known vertebrate miRNAs (Exiqon) in hybridization buffer (Roche) at 51°C for 4 h. Sections were blocked with 10% goat serum and incubated with anti-DIG alkaline phosphatase (Roche). miRNA-bound LNA probes were detected with Fast Red Substrate (Sigma). After counterstaining with DAPI, slides were mounted using FluorSave (Merck). Image acquisition was performed with an Olympus FluoView FV1000 using the TRITC filter.

Immunohistochemistry

Five-micron tissue sections were mounted on polylysine-coated glass slides (Thermo Scientific). Sections were washed in xylene and rehydrated using decreasing ethanol concentrations and finally in phosphate buffered saline (PBS). Endogenous peroxidase activity was quenched by immersing the slides in 3% hydrogen peroxide for 30 minutes. Antigen retrieval was performed using programmable pressure cooker with 'target retrieval solution', pH 6.0 (Dako). Non-specific reactivity in the tissues was blocked by incubation in 10% goat serum in PBS before incubating with the primary antibody (Anti-CEBP Beta antibody, #ab18336, Abcam) at room temperature. Unbound primary antibodies were removed before incubation with species matched secondary HRP-labeled polymer antibodies (Dako). Chromogen 3,3′-diaminobenzidine (Dako) was used as substrate for color development. Slides were counterstained with hematoxylin before dehydration and mounted with DPX (Sigma). For fluorescent immunodetection, species-specific secondary antibodies conjugated to Alexa 488/555 were used instead of HRP-labeled polymer antibodies. Sections were washed, counterstained with DAPI (100 ng/ml) and mounted using Fluorsave (Calbiochem) mounting medium. Images were acquired on a Zeiss Axioimager microscope (for bright field imaging) or on Olympus FluoView FV1000 (for fluorescent antibody detection).

Biotin-Streptavidin Pull-down

Dynabeads MyOne Streptavidin C1 (Invitrogen) were prepared according to the manufacturer's protocol. WT or mutant miR-138 promoter PCR products were amplified with 5′-UTR biotinylated primers. The binding reactions were carried out in a rotator shaker at 4°C with 2 × Binding Buffer (same as EMSA binding buffer), 10 μg Poly-dI-dC, 10 μg biotinylated DNA and 300 μg nuclear extract from U-87 MG cells. BSA-blocked beads (50 μl) were then added to the binding reaction for 15 min at 4°C. After a thorough wash in wash buffer (10 mM HEPES, 50 mM NaCl, 0.1% NP-40, 2.5 mM $MgCl_2$, 0.5 mM DTT, 10% glycerol, 1 μg/ml BSA, 1× protease inhibitor cocktail), proteins were eluted in 2 × Lammeli sample buffer at 95°C for 5 min.

Co-Immunoprecipitation (Co-IP)

Dynabeads Protein G (Invitrogen) were prepared according to the manufacturer's protocol. The binding reaction was carried out in a rotator shaker at 4°C with 2 × Binding Buffer C (HEPES pH 7.9 20 mM, NaCl 400 mM, EDTA 1mM, EGTA 0.02 mM, DTT 1 mM, PMSF 0.01 mM), 6 ug C/EBPβ antibody (sc-7962, Santa Cruz) and 300 μg nuclear extract from LAP2-FLAG expressing 293T cells. Washed beads (60 μl) were then added to the binding reaction for 1 h at 4°C. Beads were then washed for six times in wash buffer (PBST). Dynabeads were then boiled in 2x Laemmli sample buffer at 95°C for 5 min to elute proteins for western blot detection or were subjected to sample preparation for qMS-based proteomics.

Mass spectrometry analysis

For mass spectrometric analysis, proteins bound to Dynabeads were digested following the protocol described in Sundaram *et al.* (6). The peptides were injected and separated using Thermo Scientific™ Orbitrap Fusion™ Mass Spectrometer (MS) and coupled nanoUPLC Easy LC 1000 with 120 min gradient (Solvent A: 0.1% formic acid, and solvent B: 0.1% formic acid with 99.9% of acetonitrile). Peak list were generated with Proteome Discoverer (Version 1.4.1.14 Thermo Fisher Scientific), and protein identification was accomplished with Mascot 2.5.1 against Human Uniprot database with following parameters: precursor mass tolerance (MS) 25 ppm, and MS/MS 0.6 Da, three missed cleavages; static modifications of Carboamidomethyl (C), variable modifications are Biotin (K), Oxidation (M), Deamidation of (NQ). The candidates from three biological replicates presenting >2 unique peptides and >20 peptide-spectrum matches (PSM) were finally selected and subjected to experimental validation.

Statistical analysis

Error bars represent the standard deviation. Statistical significance between 2 samples was determined with two-tailed Student's *t* - test.

RESULTS

C/EBPβ is a transcriptional activator of miR-138

We analysed chromatin immunoprecipitation with sequencing (ChIP-seq) data collected by the ENCODE Consortium and observed that C/EBPβ is enriched at the miR-138-2 *locus*. This *locus* also contains a computationally predicted binding site for C/EBPβ (Figure 1A). The validity of this prediction was tested using ChIP assays in U-87 MG, which is a malignant glioma cell line. U-87 MG cells, which endogenously express high levels of miR-138, were subjected to immunoprecipitation with antibodies against C/EBPβ. We obtained significant enrichment of the DNA sequence encoding the precursor of miR-138-2 (pre-miR-138-2) with

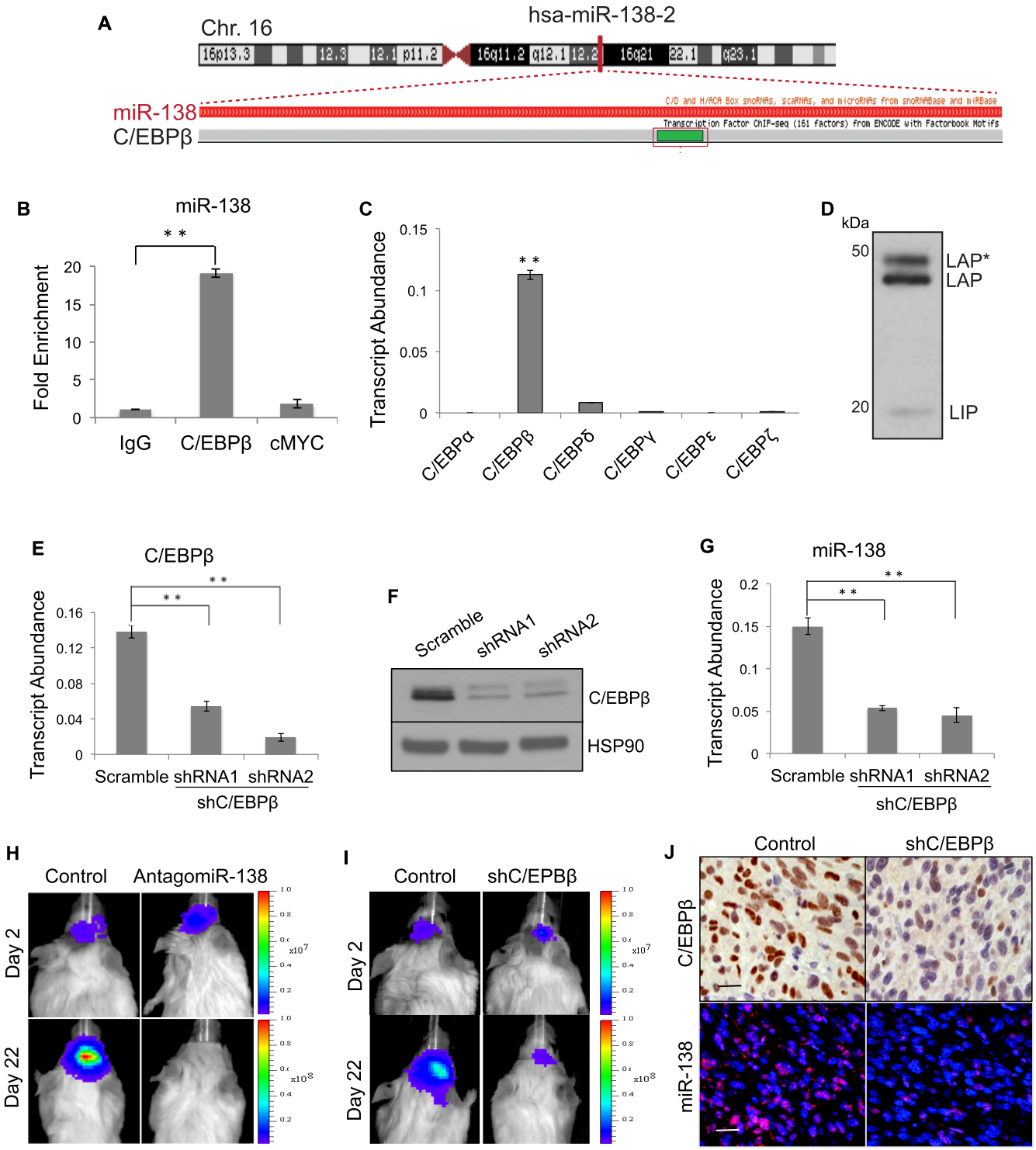

Figure 1. C/EBPβ is a transcriptional activator of miR-138: (**A**) Graphic representation of ChIP-seq analysis from ENCODE identifying a C/EBPβ binding motif. (**B**) Bar graph showing C/EBPβ occupancy on the miR-138-2 *locus*. Chromatin enrichment is expressed as fold change normalized to IgG ($n = 3$). (**C**) Transcript abundance of C/EBP family members in U-87 MG cells ($n = 3$). (**D**) Immunoblot analysis of C/EBPβ isoforms (LAP*, LAP, and LIP) in U-87 MG cells ($n = 2$). (**E**) Bar graph depicting transcript abundance of C/EBPβ upon transduction with two shRNAs ($n = 3$). (**F**) Significant down-regulation of C/EBPβ by shRNAs is confirmed by Western blot analysis. HSP90 is used as loading control ($n = 3$). (**G**) Bar graph depicting a concomitant down-regulation of miR-138 expression upon knockdown of C/EBPβ ($n = 4$). (**H**, **I**) Representative real-time images of xenografts tracked by bioluminescence at indicated time points after engraftment ($n = 15$). The bioluminescent signal measured on day 2 indicates survival of transplanted cells. Prior to implantation, cells were transduced with lentivirus encoding antagomiR-138 or shC/EBPβ ($n = 15$). (**J**) Immunohistochemical localization of C/EBPβ protein (upper panel) and expression of miR-138 detected by *in situ* hybridization (lower panel). C/EBPβ is stained brown and nuclei are stained blue (upper panel). miR-138 is stained red, and nuclei are stained blue (lower panel) Scale bar = 100 μm. Error bars represent the standard deviation. **(Student's *t*-test; $P < 0.001$).

antibodies against C/EBPβ, relative to IgG and cMYC controls (Figure 1B). The above data clearly indicate occupancy of C/EBPβ at the miR-138-2 *locus*, where it may function as a transcriptional regulator of miR-138.

To confirm that the observed enrichment on miR-138-2 in U-87 MG is solely due to C/EBPβ binding, rather than that of a related protein, we measured the transcript levels of all C/EBP family members. The C/EBP family is comprised of six proteins (α, β, γ, δ, ϵ and ζ), which interact with the CCAAT (cytidine–cytidine–adenosine–adenosine–thymidine) box motif on gene promoters. qRT-PCR data shows that C/EBPβ is the dominant isoform expressed in U-87 MG (Figure 1C). C/EBPβ is a leucine-zipper transcription factor with several N-terminally truncated isoforms. Liver-enriched activator protein (LAP) and the minor product LAP*, are transcriptional activators, whilst liver-enriched inhibitory protein (LIP), is a LAP antagonist (7,8). Increased expression of LAP/LAP* relative to LIP was demonstrated by Western blot in U-87 MG cells (Figure 1D). Having demonstrated that C/EBPβ is highly expressed in U-87 MG, where it predominantly exists as the transcriptionally active LAP isoform, we present evidence for C/EBPβ as an upstream transcriptional regulator of miR-138. Knocking down C/EBPβ using either of two different shRNAs (Figure 1E andF) resulted in a concomitant down-regulation of miR-138 (Figure 1G). These results were consistent across multiple cell lines. (Supplementary Figure S1A-S1C). In combination, the data supports a model whereby the LAP isoform of C/EBPβ, binds to the miR-138 promoter and stimulates the expression of miR-138.

To investigate the physiological role of C/EBPβ as a transcriptional activator of miR-138 in the context of malignant gliomas, we implanted U-87 MG cells expressing firefly luciferase, and either antagomiR-138 or shRNA against C/EBPβ in the striatum of immunodeficient NOD scid gamma (NSG) mice. Following stereotactic injections, Tumour growth was monitored *in vivo* using a bioluminescence imaging system. Significant inhibition of Tumour growth was apparent upon knockdown of miR-138 or C/EBPβ (Figure 1H and I). Immunohistochemical analysis of Tumour sections using anti-C/EBPβ antibody confirmed efficient knockdown of C/EBPβ (Figure 1J, upper panel). Importantly, *in situ* hybridization analysis of Tumour sections using specific probes to detect miR-138, confirmed a concomitant down-regulation of miR-138 following knockdown of C/EBPβ (Figure 1J, lower panel). Together, this suggests that C/EBPβ is an upstream regulator of miR-138 in malignant gliomas. Moreover, a decrease in cell proliferation (Supplementary Figure S2A and S2B) and an increase in caspase activity (Supplementary Figure S2C) were apparent upon knockdown of C/EBPβ. Over-expression of miR-138 resulted in the rescue of this phenotype, confirming the role of C/EBPβ-miR-138 axis in gliomagenesis (Supplementary Figure S2D and S2E). In summary, these findings add on to our proposed model, demonstrating that C/EBPβ-induced stimulation of miR-138 transcription supports cell proliferation and Tumourigenesis in the context of malignant glioma.

The trans-activator C/EBPβ directly binds to a 158 bp DNA sequence, which encodes pre-miR-138-2

Having established C/EBPβ as a trans-activator of miR-138, we sought to further characterize its role in miR-138 transcription. Six C/EBPβ binding sites were predicted within the 1.6 kb miR-138-2 *locus* (Figure 2A and Supplementary Figure S3A) by *in silico* analysis using the TRANSFAC database (9). Only one of these candidate sites, BS4, lies within the DNA sequence corresponding to pre-miR-138-2. We cloned either the entire 1.6 kb stretch of DNA, or individual deletion mutants comprising varying numbers of C/EBPβ binding sites, in a pGL4.23 luc2/minP basic vector (Figure 2B). Recombinant reporter constructs were transfected into U-87 MG cells and luciferase activity measured as a read-out of transcriptional activation. It was evident that the P4 construct, which contained just the internal BS4 site, was sufficient for C/EBPβ-mediated transcription of luciferase. Of the six constructs tested, P4 displayed the highest luciferase activity; the inclusion of additional C/EBPβ candidate sites resulted in reduced promoter activity (Figure 2B). Unlike the other five C/EBPβ binding sites, the BS4 C/EBPβ binding site in P4 resides within the DNA sequence that encodes pre-miR-138-2. We refer to this internal 14 nucleotide C/EBPβ binding site (CTATTTCACGACAC) as the 'C/EBPβ response element' (CRE) as this motif executes efficient transcription of luciferase (Figure 2B).

To further characterise the transcription of miR-138 under regulation by C/EBPβ, first we determined the optimal length of the transcription unit, which can generate pre-miR-138-2. Using 5′ Rapid Amplification of cDNA Ends (5′ RACE), we mapped the transcription start site (TSS) to 5 bp upstream of the DNA sequence corresponding to pre-miR-138-2 (Supplementary Figure S3B, S3C). Next, we generated a series of P4 deletion mutants and tested their ability to drive luciferase expression. This identified a minimal 158 bp sequence (P4.1) required for transcription; further reduction in fragment size impaired luciferase production (Figure 2C). These results were consistent in the U 251 MG glioma cell line (Supplementary Figure S4A and S4B).

Moreover, the CRE motif was critical for transcription of luciferase. Mutating CRE (Figure 2D, E) significantly decreased luciferase activity relative to the wild-type control in P4.1 (Figure 2E). Finally, knockdown of C/EBPβ substantially reduces luciferase activity driven by P4.1 (Figure 2F) and confirms that these effects are mediated through C/EBPβ as a potential transcriptional activator.

ChIP analysis was performed to provide evidence for the direct interaction of C/EBPβ with its predicted binding sites. Of the six candidates, CRE displayed the most prominent enrichment for C/EBPβ (Figure 2G). We also demonstrated the interaction using streptavidin–agarose pull-down on U-87 MG nuclear extracts incubated with biotinylated P4.1 DNA, followed by Western blotting with an anti-C/EBPβ antibody. C/EBPβ was exclusively detected following incubation with wild type P4.1 (Figure 2H). Disruption of the CRE site by mutation abrogates the interaction between C/EBPβ and P4.1, resulting in loss of the signal.

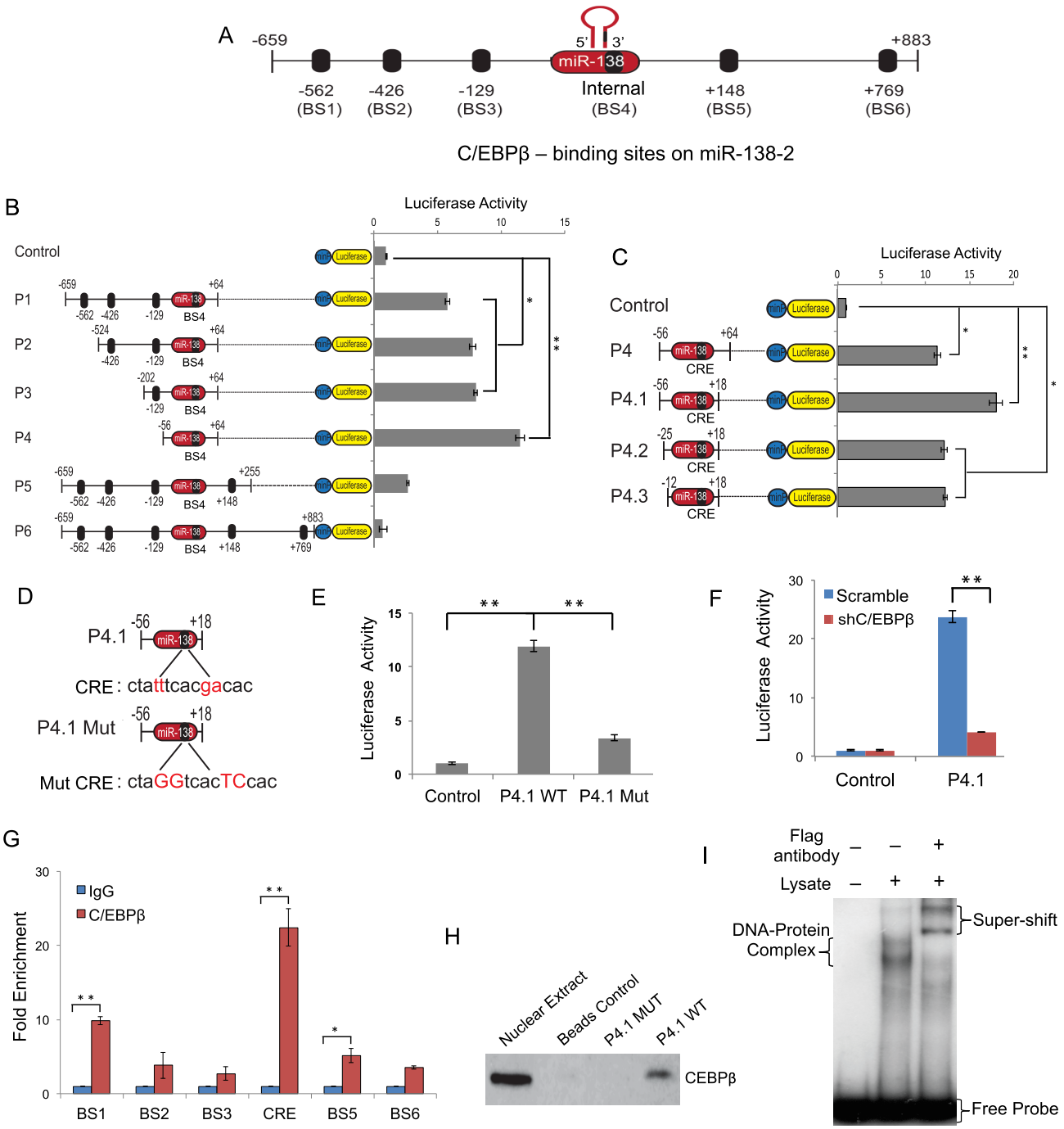

Figure 2. The trans-activator C/EBPβ directly binds to a 158 bp DNA sequence, which encodes pre-miR-138-2: (**A**) Schematic representation of six putative C/EBPβ binding sites on the miR-138-2 *locus* predicted by TRANSFAC database. (**B**) Schematic illustrating deletion mutants of the miR-138 promoter and their associated normalized luciferase activities ($n = 3$). P4, with only one C/EBPβ binding site, was sufficient for C/EBPβ-mediated luciferase activity. We refer to this C/EBPβ- motif within the pre-miR-138-2 sequence as the 'C/EBPβ response element' (CRE). (**C**) Schematic illustrating deletion mutants of the P4 clone and their associated normalized luciferase activity ($n = 3$). P4.1, with a short 158 bp pre-miR-138-2 sequence (with the embedded CRE) is sufficient for the binding of C/EBPβ and transcriptional activation of luciferase. (**D**) Schematic representation of WT and mutant CRE within the miR-138 precursor sequence. (**E**) Mutant CRE abolishes C/EBPβ binding leading to a decrease in luciferase activity compared with WT CRE. Bar graph indicates fold change of luciferase activity normalized to Renilla luminescence ($n = 3$). (**F**) Luciferase assay data for the P4.1 construct in response to treatment with either shC/EBPβ or control shRNA ($n = 3$). (**G**) ChIP analysis for C/EBPβ occupancy at the six predicted C/EBPβ binding sites on miR-138 *locus* ($n = 2$). (**H**) Western blot analysis of nuclear extracts from U-87 MG cells incubated with biotinylated 158 bp pre-miR-138-2 sequence (with the embedded mutant or WT CRE), subjected to streptavidin-agarose pull-down assay. Nuclear Extract and Bead Controls are used as positive and negative controls for C/EBPβ detection, respectively ($n = 3$). (**I**) Electrophoretic mobility shift assay on nuclear lysates from 293T cells overexpressing C/EBPβ-Flag incubated with radiolabeled 158 bp pre-miR-138 sequence. The specific DNA/protein complex (lane 2) is super-shifted upon addition of FLAG antibody (lane 3) in an electrophoretic mobility shift assay ($n = 3$). Error bars represent the standard deviation. (Student's *t*-test; *[$P < 0.05$], **[$P < 0.001$])

We provide further evidence for the direct binding of C/EBPβ to P4.1 using electrophoretic mobility shift assays (EMSA). Nuclear lysates from 293T cells overexpressing the FLAG-tagged C/EBPβ isoform LAP were incubated with wild-type ^{32}P-radiolabeled P4.1 and subjected to EMSA. Formation of a specific DNA-protein complex and supershift of the same using an anti-FLAG antibody confirmed the specificity of binding (Figure 2I). These results demonstrate the interaction of C/EBPβ with P4.1 via CRE, validating CRE as a direct binding site for C/EBPβ. Furthermore, conservation of the CRE element was observed in all vertebrate species studied (Supplementary Figure S5). This suggests that the C/EBPβ-CRE interaction has an important functional role, and therefore retained by natural selection across vertebrate evolution.

Binding of C/EBPβ to the conserved CRE initiates miR-138 transcription

In order to validate luciferase output as an accurate readout of miR-138 transcription, we repeated the above experiments in 293T cells, which lack endogenous expression of miR-138. In line with our observations in glioma cell lines, it was evident that the P4 construct, which contained just the internal CRE site, was sufficient for C/EBPβ-mediated transcription of luciferase and displayed the highest luciferase output (Figure 3A). miR-138 expression was also directly quantified using qRT-PCR and observed to be comparable to the luciferase data and inclusion of additional C/EBPβ candidate sites resulted in reduced promoter activity (Figure 3B). Similarly, the 158 bp sequence in P4.1 was found to be sufficient for transcription of luciferase (Figure 3C) and activation of miR-138 expression (Figure 3D). Mutating CRE in P4.1 or in the native context on P6 (Figure 3E and F) significantly decreased luciferase activity and miR-138 expression relative to the wild-type control (Figure 3G and H). Our luciferase assay data demonstrate that this short segment of DNA, containing a single C/EBPβ binding site, allows for maximal promoter activity. The observation that this transcription unit also produces optimal miR-138 output in 293T cells further demonstrates that C/EBPβ functions as a transcriptional regulator positioned internal to the miR-138-2 locus. Taken together, the above data suggest that a short 158 bp DNA sequence encoding pre-miR-138-2 containing CRE is necessary and sufficient for the transcriptional activation of miR-138.

Transcription of miR-138 is independent of RNA Polymerase II

To understand the role of C/EBPβ in miR-138 transcription, we set out to characterise the type of promoter responsible for miR-138 transcription. The small size and self-sufficiency of the miR-138 transcription unit caught our attention. By contrast, the miR-21 transcription unit spans several kilobases of DNA (Figure 4A). We were interested to study the organisation of promoter elements within P4.1 and how this enables transcription from a 158 bp minimal sequence. The TATA box motif, initiator (Inr) element, and DTIE (10) are absent in P4.1, suggesting that the transcription of miR-138 may be independent of RNA Polymerase II (Pol II) (Figure 4A). We performed ChIP assays to test our hypothesis on the Pol II independent transcription of miR-138. Chromatin from U-87 MG cells was subjected to immunoprecipitation with the 8WG16 and N20 antibodies, which target epitopes at the C-terminal domain and N-terminus of RNA Pol II respectively. Significant enrichment of RNA Pol II subunits was evident on the miR-21 *locus*, but not on the miR-138-2 *locus* (Figure 4B). Enrichment was absent, from the promoter of the Pol III-transcribed miR-886 and tRNA-Glu *loci* (Figure 4B).

Moreover, transcription of miR-138 was found to be resistant to the treatment with α-amanitin (Figure 4C) and 5,6-dichloro-1-β-d-ribofuranosylbenzimidazole (DRB), both of which inhibit RNA Pol II (Figure 4D). We observed a significant reduction in transcript abundance of miR-106a, miR-21 and cMyC upon α-amanitin or DRB treatment, indicating that the treatment successfully inhibited Pol II. miR-886, tRNA-Glu and 5s rRNA, which are known to be Pol III-transcribed, were also used as negative controls. These transcripts did not change in abundance upon α-amanitin or DRB treatment (Figure 4C and D). No significant change in miR-138 transcript abundance was observed upon treatment with a-amanitin or DRB (Figure 4C and D). These results confirm that, unlike majority of miRNAs, transcription of miR-138 is independent of RNA Pol II. Moreover, ChIP-seq data from the ENCODE project also shows that K562 and HepG2 cell lines, both of which express miR-138 (Figure 4E), lack Pol II enrichment at the miR-138-2 locus (Figure 4F, upper panel). This enrichment is clearly present at the miR-21 locus, which is a known Pol II-driven transcription unit (Figure 4F, lower panel). Taken together, all the above confirm Pol II-independent transcription of miR-138.

C/EBPβ co-ordinates recruitment of TFIIIC and mediates transcription of miR-138 by RNA Polymerase III

Sequence analysis of P4.1 identified the presence of the A- and B-box promoter elements, which are characteristic of RNA Polymerase III (Pol III) promoters (Figure 5A). This prompted us to investigate the occupancy of RNA Pol III on miR-138-2 *locus*. Chromatin from U-87 MG cells was subjected to immunoprecipitation with antibodies against the RNA Pol III subunits PolR3C, PolR3D and PolR3E. The miR-138-2 *locus* showed significant enrichment of all three subunits. The promoters of the established Pol III products tRNA-Glu and miR-886 exhibit similar enrichment (11,12). Enrichment was absent, from the promoter of the Pol II-transcribed miR-21 *locus* (Figure 5B). Moreover, cells were treated with the Pol III inhibitor CAS 577784-91-9, which is a specific inhibitor of RNA Pol III, following which transcript abundance was tested for miR-106a, miR-21 and cMyc (all Pol II-transcribed genes used as negative controls). Transcript levels were also measured in three positive controls – miR-886, tRNA-Glu and 5s rRNA. We observed a significant reduction in miR-138 transcript abundance upon treatment with CAS 577784-91-9, indicating that miR-138 transcription requires RNA Pol III (Figure 5C). Furthermore, exogenous expression of miR-138 PCR product (P4.1) in 293T cells followed by treatment with Pol-III inhibitor, CAS 577784-91-9 results in a significant de-

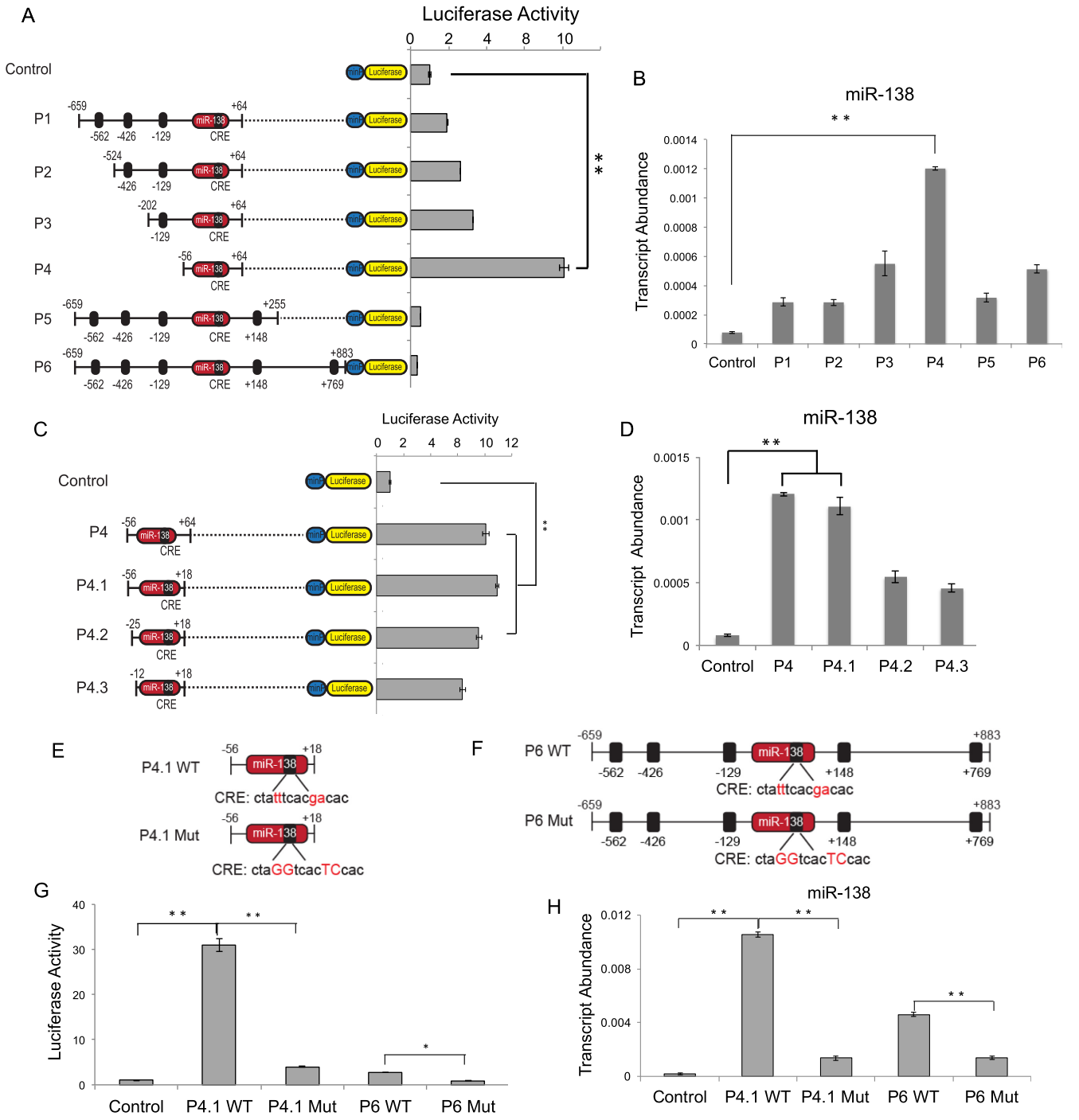

Figure 3. Binding of C/EBPβ to the Conserved CRE initiates miR-138 transcription: (**A**) Schematic illustrating deletion mutants of the miR-138 promoter and their associated normalized luciferase activities in 293T cells ($n = 3$). Note, that P4, with only one C/EBPβ binding site (CRE), was sufficient for C/EBPβ-mediated luciferase activity. (**B**) Transcript abundance of miR-138 in 293T cells upon transfection with the indicated deletion mutants ($n = 3$). Note, that P4, with only one C/EBPβ binding site, was sufficient for C/EBPβ-mediated *miR-138* transcriptional activity. (**C**) Schematic illustrating deletion mutants of the P4 clone and their associated normalized luciferase activity (n = 3). P4.1, with a short 158 bp pre-miR-138-2 sequence (with the embedded CRE) is sufficient for the binding of C/EBPβ and transcriptional activation of luciferase. (**D**) Transcript abundance of miR-138 in 293T cells upon transfection with the indicated P4 deletion mutants ($n = 3$). (**E**) Schematic representation of WT and mutant CRE in P4.1. (**F**) Schematic representation of WT and mutant CRE in P6. (**G**) Mutant CRE abolishes C/EBPβ binding leading to a decrease in luciferase activity compared with WT CRE ($n = 3$). Bar graph indicates fold change of luciferase activity normalized to Renilla luminescence. (**H**) Transcript abundance of miR-138 in 293T cells upon transfection with the indicated P4.1 or P6 WT and deletion mutants ($n = 3$). Error bars represent the standard deviation. (Student's *t*-test; *[$P < 0.05$], **[$P < 0.001$]).

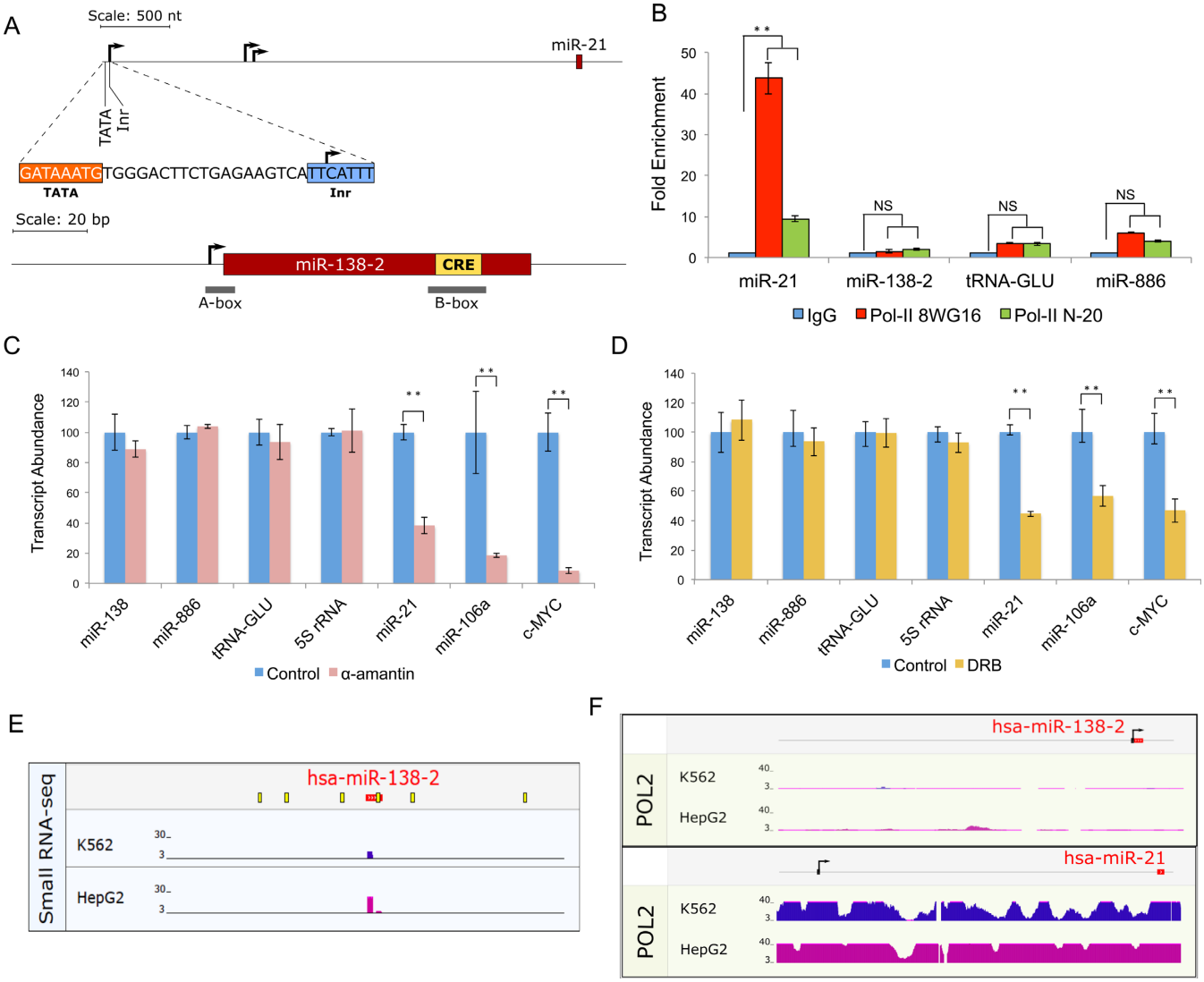

Figure 4. Transcription of miR-138 is independent of RNA Polymerase II: (**A**) Schematic representation of miR-21 and miR-138 genomic *loci* with their associated promoter elements. (**B**) ChIP analysis for RNA Pol II subunits occupancy on miR-21, miR-138, miR-886 and tRNA-GLU *loci* ($n = 4$). Bar graph depicts fold enrichment of RNA Pol II subunits on the *loci*. (**C**, **D**) Quantitative real time PCR analysis on cells treated with α-amanitin or DRB, which are inhibitors of RNA Pol II, along with DMSO as a control ($n = 3$). (**E**) UCSC Genome Browser view showing Illuminia GAIIx small RNA-seq data for the miR-138-2 locus in the indicated cancer cell lines. Data was obtained from the ENCODE/Cold Spring Harbor Lab track for short RNAs treated with Alkaline Phosphatase. Signal intensity (y-axis) shows density of mapped reads on plus strand. (**F**) UCSC Genome Browser view showing ChIP-seq data for POL2 (Pol II) in indicated cancer cell lines for miR-21 and miR-138. Signal intensity (y-axis) is a representation of enrichment for transcription factor binding based on the number of overlapping ChIP DNA fragments at each nucleotide position. Error bars represent the standard deviation. (Student's *t*-test; *[$P < 0.05$], **[$P < 0.001$])

crease in pre-miR-138-2 (Supplementary Figure S6). However, transcription was not affected upon treatment with α-amanitin. In summary, these results suggest that miR-138 belongs to a cohort of small RNAs, which are transcribed by RNA Pol III.

In an attempt to identify the role of C/EBPβ in RNA Pol III mediated transcription of miR-138, using specific antibodies against C/EBPβ we performed an immunoprecipitation (IP) on nuclear lysates from 293T cells over-expressing C/EBPβ. The product from IP was subjected to mass spectrophotometric (MS) analysis, to identify the potential interacting partners of C/EBPβ. Analysis of the IP-MS data and gene ontology analysis resulted in the identification of General Transcription Factor 3C polypeptide 3 (GTF3C3), as one of the specific interacting partners of C/EBPβ (Figure 5D). Western blot of the immunoprecipitate using TFIIIC102 antibody further confirms the interaction of C/EBPβ with TFIIIC102 (Figure 5E). GTF3C3 encodes one of the subunits of the transcription factor 3C (TFIIIC) complex, which is required to position the RNA Pol III at the gene promoter and initiate transcription (13,14). TFIIIC is known to bind the intragenic *cis*-acting promoter elements, the A and B boxes and promotes the binding of TFIIIB upstream of the TSS to initiate transcription (15). ChIP assays using antibodies against TFIIIC and TFIIIB subunits revealed significant enrichment of TFI-

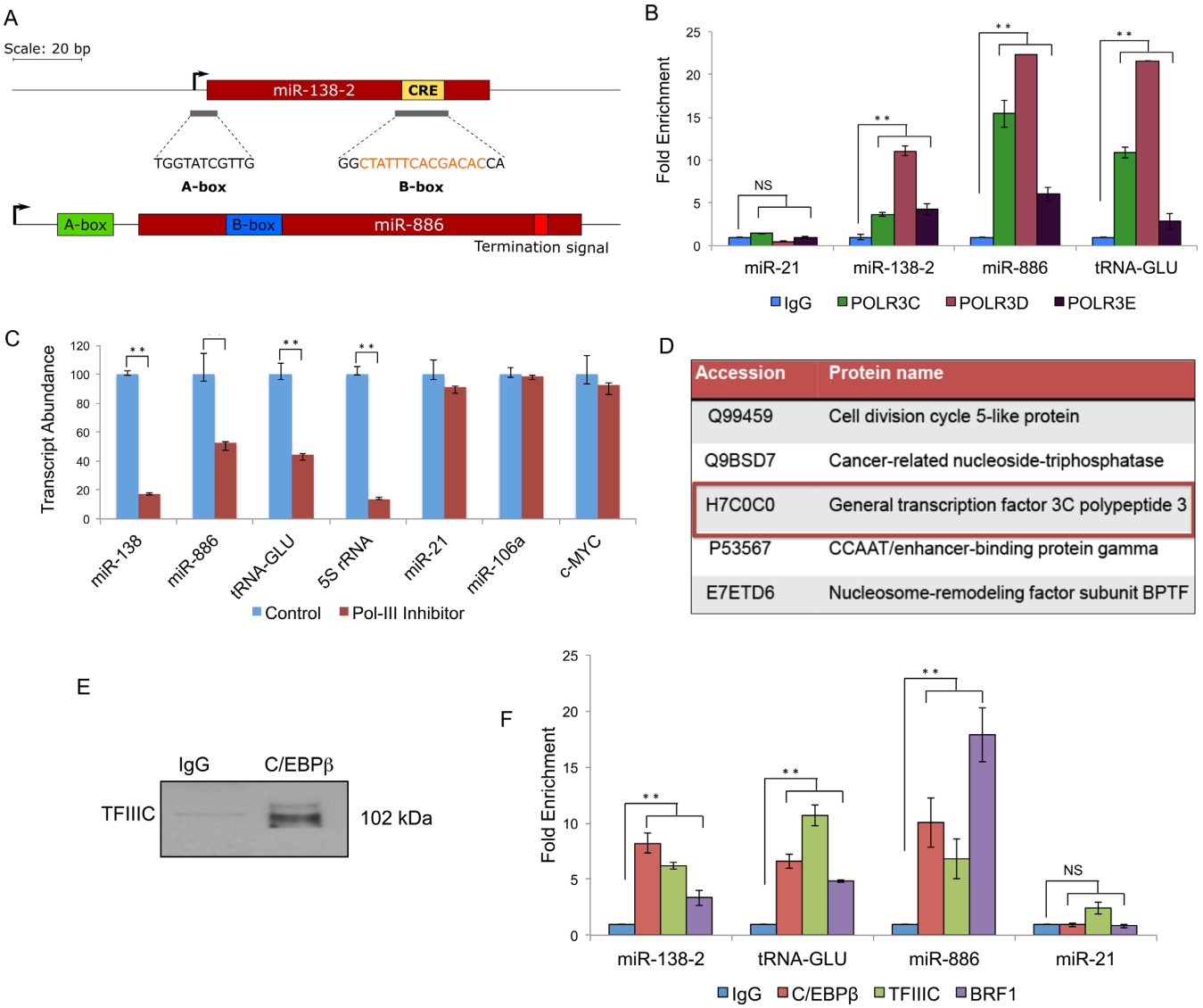

Figure 5. C/EBPβ recruits TFIIIC and mediates transcription of miR-138 by RNA Polymerase III: (**A**) Schematic representation of miR-138 and miR-886 genomic *loci* with the promoter elements. (**B**) ChIP analysis for RNA Pol III subunits occupancy on miR-21, miR-138, miR-886 and tRNA-Glu *loci* ($n = 4$). (**C**) Quantitative real time PCR analysis of miR-138 and miR-886 on cells treated with CAS 577784-91-9, which is a specific inhibitor of RNA Pol III or DMSO as a control ($n = 3$). (**D**) Selected list of C/EBPβ-interacting candidates from IP-MS analysis, which includes TFIIIC. (**E**) IP-Western blot depicting direct interaction of C/EBPβ with TFIIIC ($n = 2$). (**F**) ChIP analysis for C/EBPβ, BRF1 and TFIIIC occupancy on miR-21, miR-138, miR-886 and tRNA-Glu *loci* ($n = 4$). Error bars represent the standard deviation. (Student's *t*-test; *[$P < 0.05$], **[$P < 0.001$])

IIC102 and BRF1, which is part of the TFIIIB complex, on miR-138 *locus,* but not on miR-21 promoter, thereby indicating specific association with RNA Pol III complex (Figure 5F). Significant enrichment of TFIIIC102, BRF1 and C/EBPβ were also observed on miR-886 and tRNA-Glu *loci*, which are transcribed by RNA Pol III (Figure 5F). The above results suggest a vital role for C/EBPβ in recruitment of components of the RNA Pol III transcriptional complex.

C/EBPβ orchestrates recruitment of components of the RNA Pol III transcriptional complex

Here we used miR-886 and tRNA-Glu as our positive controls with reference to RNA Pol III-dependent transcription. As expected, we observed enrichment of PolR3D and TFIIIC on both miR-886 and tRNA-Glu *loci* (Figure 5B and F). However, we were surprised to also observe C/EBPβ enrichment on both miR-886 and tRNA-Glu *loci* in U87-MG cells, as well as multiple cancer cell lines (Figure 6A–C). We speculate that C/EBPβ may be a transcriptional co-activator for a cohort of RNA Pol III transcribed small RNAs, including miR-138 and potentially co-ordinates the recruitment of components of RNA Pol III transcription complex. To address this hypothesis, we investigated the expression of miR-886 and tRNA-GLU expression upon knockdown of C/EBPβ. Similar to miR-138 we observed a significant down-regulation of miR-886 and tRNA-GLU upon knockdown of C/EBPβ (Figure 6D–F). Finally, ChIP assays using TFIIIC, BRF1 and PolR3D antibodies on miR-138 locus indicates a significant decrease

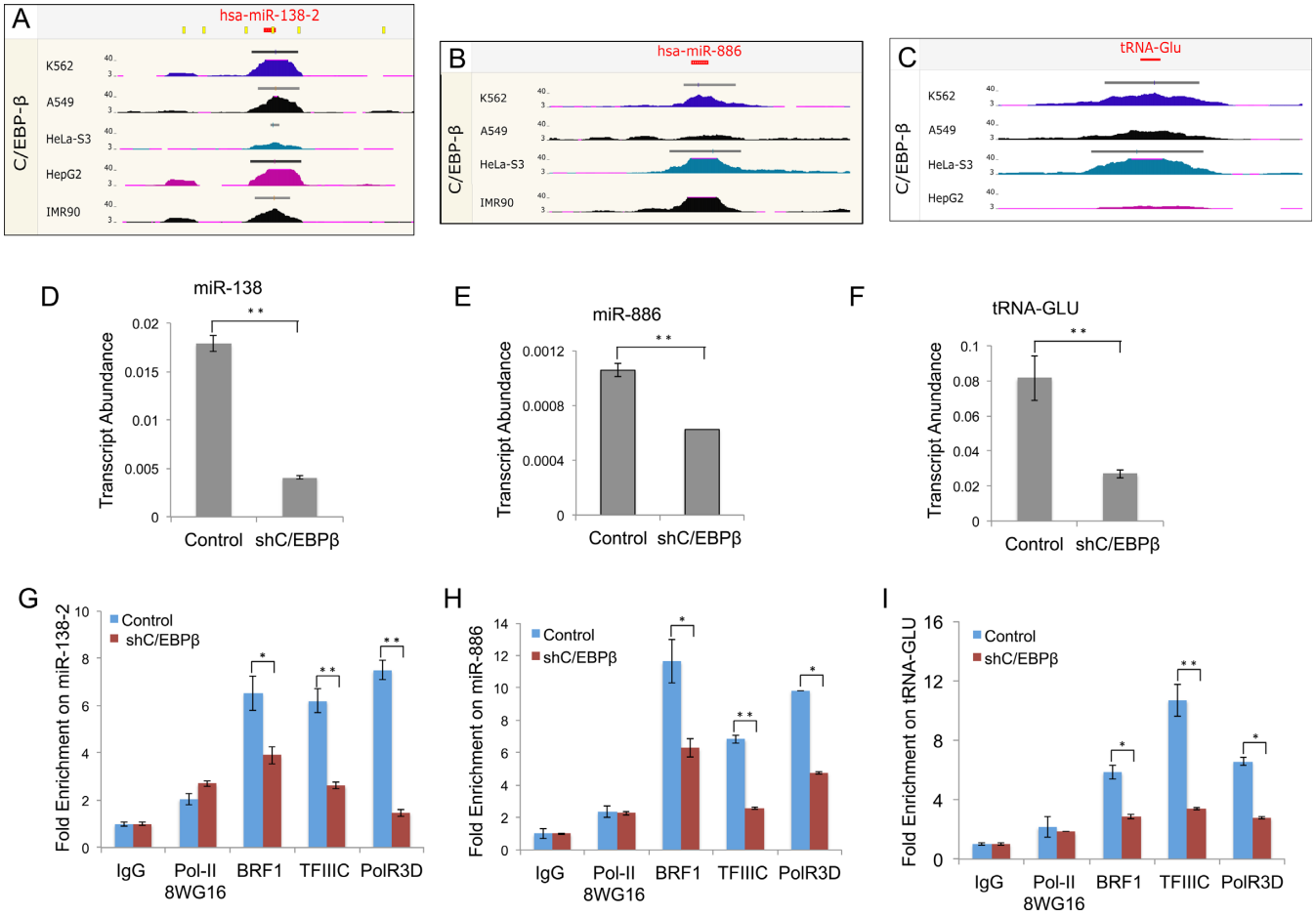

Figure 6. C/EBPβ orchestrates recruitment of components of the RNA Pol III transcriptional complex: (**A**) UCSC Genome Browser view showing ChIP-seq data for C/EBP-β in the indicated cancer cell lines on miR-138 locus. Signal intensity (y-axis) is a representation of enrichment for transcription factor binding based on the number of overlapping ChIP DNA fragments at each nucleotide position. (**B**) UCSC Genome Browser view showing ChIP-seq data for C/EBP-β in the indicated cancer cell lines on miR-886 locus. (**C**) UCSC Genome Browser view showing ChIP-seq data for C/EBP-β in the indicated cancer cell lines on tRNA-GLU locus. (**D**) Bar graph depicting a concomitant down-regulation of miR-138 expression upon knockdown of C/EBPβ ($n = 5$). (**E**) Bar graph depicting a concomitant down-regulation of miR-886 expression upon knockdown of C/EBPβ ($n = 3$). (**F**) Bar graph depicting a concomitant down-regulation of tRNA-GLU expression upon knockdown of C/EBPβ ($n = 3$). (**G**) ChIP analysis indicates a significant decrease in PolR3D, BRF1 and TFIIIC occupancy on miR-138 locus upon C/EBPβ knockdown. (**H**) ChIP analysis indicates a significant decrease in PolR3D, BRF1 and TFIIIC occupancy on miR-886 locus upon C/EBPβ knockdown ($n = 2$). (**I**) ChIP analysis indicates a significant decrease in PolR3D, BRF1 and TFIIIC occupancy on tRNA-GLU locus upon C/EBPβ knockdown. Error bars represent the standard deviation. (Student's *t*-test; *[$P < 0.05$], **[$P < 0.001$])

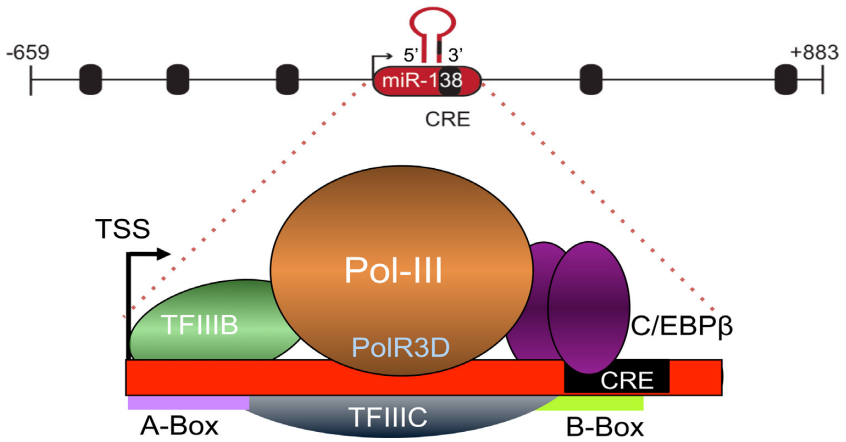

Figure 7. Schematic representation of miR-138 transcriptional regulation: C/EBPβ binds to the CRE which overlaps with B-box element, co-ordinates recruitment of TFIIIC and steers transcription of miR-138 by RNA Pol III.

in the occupancy of all three subunits upon knockdown of C/EBPβ (Figure 6G). We observed a similar result on miR-886 and tRNA-GLU loci (Figure 6H and I). Together, this suggests that C/EBPβ is a transcriptional co-activator and may co-ordinate recruitment of components of RNA Pol III transcriptional complex for a cohort of RNA Pol III transcribed small RNAs, including miR-138.

DISCUSSION

MicroRNA-138 targets multiple pro-apoptotic genes and tumour suppressors, and is a known pro-survival oncomiR in glioma stem cells (2). Cancer-associated miRNAs have been the subject of much research; tremendous progress has been made towards our understanding of their expression profiles, roles in pathology, as well as the potential for miRNA-based targeted therapies (16–18). However, factors controlling the transcriptional activation of many miRNAs still remain poorly characterized largely due to a lack of experimental validation. Here, we identify C/EBPβ as an upstream transcriptional activator of miR-138. We show that a short 158 bp DNA sequence functions as a self-contained transcription unit for pre-miR-138-2, and that this contains a single predicted binding site for C/EBPβ – the C/EBPβ response element (CRE). Using ChIP analysis, streptavidin-agarose pull-down, and EMSA assays, we demonstrate that C/EBPβ binds directly to CRE. It is through this direct interaction that C/EBPβ drives transcription of the oncomiR miR-138.

The role of C/EBPβ in gliomagenesis and its increased expression has been documented in malignant gliomas. Knockdown of C/EBPβ is known to impede Tumour formation (19,20). Understanding the molecular mechanisms by which C/EBPβ stimulates miR-138 transcription thereby advances our knowledge of the development and progression of gliomas. The identification of the CRE sequence as a necessary and sufficient component in C/EBPβ-mediated up-regulation of miR-138 is of particular significance; the C/EBPβ-CRE interaction may prove a worthwhile candidate in the development of targeted anticancer therapies.

Our study of the 158 bp transcription unit encoding pre-miR-138-2 also represents the first comprehensive demonstration of miRNA expression under regulation by an RNA Polymerase III promoter. MicroRNAs are reported to undergo transcription by either RNA Polymerase II or RNA Polymerase III (21,22). While there have been earlier reports on Pol III-transcribed miRNAs, the transcription products in each case have been subsequently found to represent other RNA species. One group identified miRNA clusters synthesized by RNA Pol III from A- and B-boxes in *Alu* sequences on chromosome 19 (22). In another report, the authors describe eleven miRNAs or miRNA clusters occupied by Pol III (23). However, Canella *et al.*, described that, with the exception of miR-565, none of the other miRNA *loci* or clusters displayed enrichment for BDP1, BRF1 or POLR3D. The miR-565 *locus* was subsequently also found to correspond to a tRNA (11).

The analysis of another *locus* formerly designated as a miRNA, miR-886, presents the tantalising prospect that our findings on the C/EBPβ-mediated regulation of miR-138 may apply more broadly to other Pol III promoters. miR-886, now classified as a vault RNA, VTRNA2 (24,25), is transcribed by RNA Pol III and processed by a Drosha independent, Dicer dependent mechanism (26). We speculate that C/EBPβ may be a transcriptional co-activator for a cohort of RNA Pol III transcribed small RNAs, including miR-138.

In summary, we report that C/EBPβ is a direct transcriptional activator of miR-138 in the context of malignant glioma, and acts through an internal CRE site to induce miR-138 transcription. C/EBPβ binds to CRE, which overlaps with the B-box *cis*-acting element and co-ordinates the binding of TFIIIC to the B-box to initiate RNA Pol III-mediated transcription of miR-138 (Figure 7). Transcriptional activation is induced through the RNA Pol III complex, involving the recruitment of key Pol III transcription initiation factors to the pre-miR-138-2 locus. This C/EBPβ-mediated stimulation of RNA Pol III transcription may be a general feature of a subset of Pol III promoters with specific ramifications in pathological conditions.

ACCESSION NUMBERS

https://repository.jpostdb.org/entry/JPST000274.

SUPPLEMENTARY DATA

Supplementary Data are available at NAR Online.

FUNDING

Biomedical Research Council of Singapore; A*STAR Investigatorship award (to P.S.). Funding for open access charge: Institutional Core Funding.
Conflict of interest statement. None declared.

REFERENCES

1. Bush,N.A., Chang,S.M. and Berger,M.S. (2016) Current and future strategies for treatment of glioma. *Neurosurg Rev.*, **40**, 1–14.
2. Chan,X.H., Nama,S., Gopal,F., Rizk,P., Ramasamy,S., Sundaram,G., Ow,G.S., Ivshina,A.V., Tanavde,V., Haybaeck,J. *et al.* (2012) Targeting glioma stem cells by functional inhibition of a prosurvival oncomiR-138 in malignant gliomas. *Cell Rep.*, **2**, 591–602.
3. Lagos-Quintana,M., Rauhut,R., Yalcin,A., Meyer,J., Lendeckel,W. and Tuschl,T. (2002) Identification of tissue-specific microRNAs from mouse. *Curr. Biol.*, **12**, 735–739.
4. Weber,M.J. (2005) New human and mouse microRNA genes found by homology search. *FEBS J.*, **272**, 59–73.
5. Obernosterer,G., Leuschner,P.J., Alenius,M. and Martinez,J. (2006) Post-transcriptional regulation of microRNA expression. *RNA*, **12**, 1161–1167.
6. Sundaram,G.M., Ismail,H.M., Bashir,M., Muhuri,M., Vaz,C., Nama,S., Ow,G.S., Vladimirovna,I.A., Ramalingam,R., Burke,B. *et al.* (2017) EGF hijacks miR-198/FSTL1 wound-healing switch and steers a two-pronged pathway toward metastasis. *J. Exp. Med.*, **214**, 2889–2900.
7. Zahnow,C.A. (2009) CCAAT/enhancer-binding protein beta: its role in breast cancer and associations with receptor tyrosine kinases. *Expert Rev. Mol. Med.*, **11**, e12.
8. Ramji,D.P. and Foka,P. (2002) CCAAT/enhancer-binding proteins: structure, function and regulation. *Biochem. J.*, **365**, 561–575.
9. Matys,V., Fricke,E., Geffers,R., Gossling,E., Haubrock,M., Hehl,R., Hornischer,K., Karas,D., Kel,A.E., Kel-Margoulis,O.V. *et al.* (2003) TRANSFAC: transcriptional regulation, from patterns to profiles. *Nucleic Acids Res.*, **31**, 374–378.

10. Marbach-Bar,N., Bahat,A., Ashkenazi,S., Golan-Mashiach,M., Haimov,O., Wu,S.Y., Chiang,C.M., Puzio-Kuter,A., Hirshfield,K.M., Levine,A.J. *et al.* (2016) DTIE, a novel core promoter element that directs start site selection in TATA-less genes. *Nucleic Acids Res.*, **44**, 1080–1094.
11. Canella,D., Praz,V., Reina,J.H., Cousin,P. and Hernandez,N. (2010) Defining the RNA polymerase III transcriptome: Genome-wide localization of the RNA polymerase III transcription machinery in human cells. *Genome Res.*, **20**, 710–721.
12. White,R.J. (2011) Transcription by RNA polymerase III: more complex than we thought. *Nat. Rev. Genet.*, **12**, 459–463.
13. Lassar,A.B., Martin,P.L. and Roeder,R.G. (1983) Transcription of class III genes: formation of preinitiation complexes. *Science*, **222**, 740–748.
14. Dean,N. and Berk,A.J. (1988) Ordering promoter binding of class III transcription factors TFIIIC1 and TFIIIC2. *Mol. Cell. Biol.*, **8**, 3017–3025.
15. Kassavetis,G.A., Riggs,D.L., Negri,R., Nguyen,L.H. and Geiduschek,E.P. (1989) Transcription factor IIIB generates extended DNA interactions in RNA polymerase III transcription complexes on tRNA genes. *Mol. Cell. Biol.*, **9**, 2551–2566.
16. Mendes,N.D., Freitas,A.T. and Sagot,M.F. (2009) Current tools for the identification of miRNA genes and their targets. *Nucleic Acids Res.*, **37**, 2419–2433.
17. Mendell,J.T. and Olson,E.N. (2012) MicroRNAs in stress signaling and human disease. *Cell*, **148**, 1172–1187.
18. Cheng,C.J., Bahal,R., Babar,I.A., Pincus,Z., Barrera,F., Liu,C., Svoronos,A., Braddock,D.T., Glazer,P.M., Engelman,D.M. *et al.* (2015) MicroRNA silencing for cancer therapy targeted to the tumour microenvironment. *Nature*, **518**, 107–110.
19. Aguilar-Morante,D., Cortes-Canteli,M., Sanz-Sancristobal,M., Santos,A. and Perez-Castillo,A. (2011) Decreased CCAAT/enhancer binding protein beta expression inhibits the growth of glioblastoma cells. *Neuroscience*, **176**, 110–119.
20. Carro,M.S., Lim,W.K., Alvarez,M.J., Bollo,R.J., Zhao,X., Snyder,E.Y., Sulman,E.P., Anne,S.L., Doetsch,F., Colman,H. *et al.* (2010) The transcriptional network for mesenchymal transformation of brain tumours. *Nature*, **463**, 318–325.
21. Ha,M. and Kim,V.N. (2014) Regulation of microRNA biogenesis. *Nat. Rev. Mol. Cell Biol.*, **15**, 509–524.
22. Borchert,G.M., Lanier,W. and Davidson,B.L. (2006) RNA polymerase III transcribes human microRNAs. *Nat. Struct. Mol. Biol.*, **13**, 1097–1101.
23. Ozsolak,F., Poling,L.L., Wang,Z., Liu,H., Liu,X.S., Roeder,R.G., Zhang,X., Song,J.S. and Fisher,D.E. (2008) Chromatin structure analyses identify miRNA promoters. *Genes Dev.*, **22**, 3172–3183.
24. Nandy,C., Mrazek,J., Stoiber,H., Grasser,F.A., Huttenhofer,A. and Polacek,N. (2009) Epstein-barr virus-induced expression of a novel human vault RNA. *J. Mol. Biol.*, **388**, 776–784.
25. Stadler,P.F., Chen,J.J., Hackermuller,J., Hoffmann,S., Horn,F., Khaitovich,P., Kretzschmar,A.K., Mosig,A., Prohaska,S.J., Qi,X. *et al.* (2009) Evolution of vault RNAs. *Mol. Biol. Evol.*, **26**, 1975–1991.
26. Persson,H., Kvist,A., Vallon-Christersson,J., Medstrand,P., Borg,A. and Rovira,C. (2009) The non-coding RNA of the multidrug resistance-linked vault particle encodes multiple regulatory small RNAs. *Nat. Cell. Biol.*, **11**, 1268–1271.